Mechanism of nanoparticle manipulation by scanning tunnelling microscopy

J Grobelny[1,2]**, D-H Tsai**[1,3]**, D-I Kim**[1]**, N Pradeep**[1]**, R F Cook**[1] **and M R Zachariah**[1,3]

[1] National Institute of Standards and Technology, Gaithersburg, MD 20899, USA
[2] University of Lodz, 90-236 Lodz, Poland
[3] University of Maryland, College Park, MD 20740, USA

E-mail: jaroslaw.grobelny@nist.gov

Abstract
Scanning tunnelling microscopy (STM) imaging was performed on gold
surfaces with a large coverage of monodispersed silver nanoparticles
soft-landed on the surface from the gas phase. In both ambient and ultra-high
vacuum conditions, STM scanning was found to displace the particles out of
the scanning area, due to weak adhesion of the particles to the substrate
surface. Calculations based on contact mechanics and electrostatics show that
the particles can overcome the force of adhesion to the surface and jump onto
the STM tip beyond the tunnelling distance. The observation provides the
possibility for patterning or arranging nanoparticles on a surface, which is
demonstrated, and offers the potential for a multiplexed approach to create
very precise surface patterns and particle arrangements.

(Some figures in this article are in colour only in the electronic version)

1. Introduction

Nanoscale engineering using nanoparticle assembly, manipulation and lithography offers tremendous opportunities for developing new devices in a variety of applications [1, 2]. Among the various nanoparticle lithography methods [3, 4] scanning probe techniques [5, 6] are simple, inexpensive and capable of direct patterning on a surface. Manipulation and lithography require a good understanding of the nature of interaction between the particles and the underlying substrate material. A major concern in this area is the control of particle–substrate adhesion, which is known to depend on the details of synthesis and deposition [7]. Atomic force microscopy (AFM) has been a powerful tool in imaging and lithography of nanoparticles [8, 9]. In this paper we present results indicating that nanoparticles were removed by a scanning STM tip from the substrate. The phenomenon is explained on the basis of dielectrophoresis and strength of the adhesive contact of a particle to the substrate. The particles were 'soft-landed' on the surface, minimizing adhesion to the surface and enabling nanoparticle lithography. We demonstrate that the approach is highly controllable and sufficient to create precise particle-free patterns on a substrate.

2. Experiment

Substrates were prepared with a uniform coverage of Ag nanoparticles by aerosol deposition. The particles were synthesized by two different methods from the gas phase: (1) evaporation–condensation [10] and (2) spray pyrolysis [11]. In method (1), Ag powder (purity 99.99%) was heated at 1140 °C in a tube furnace in a flow of high-purity nitrogen. The resulting Ag vapour was subsequently condensed to nanoparticles in a condensation flow-tube. In method (2), a $AgNO_3$ (99+%, Aldrich)-water solution was atomized into droplets and passed to a 850 °C flow reactor with nitrogen. At this temperature the metal nitrate was converted to pure Ag aerosol. Both methods yielded a rather wide particle size distribution and, in the case of evaporation–condensation, particles were in a highly aggregated state. To deal with these two problems, we used ion-mobility separation of charged particles using a differential mobility analyser (DMA) to create a narrow size distribution [12, 13]. The DMA, which operates like a band-pass filter, provides a source of singly charged monodispersed aerosol. These aerosol particles (in 1 lpm of gas) were then mixed with a flow of H_2 (0.02 lpm) and delivered to a second tube furnace at 600–800 °C, for
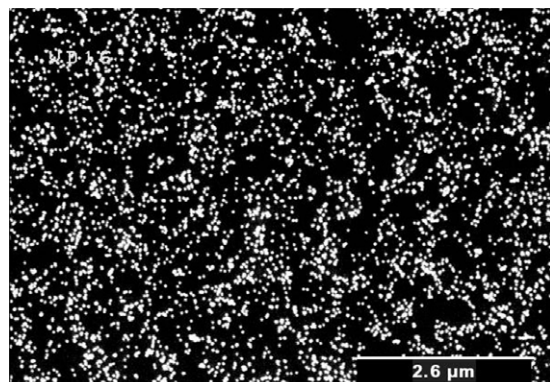
Figure 1. SEM image of Ag nanoparticles on an Au substrate.

sintering the aggregates into spherical nanoparticles. These particles were subsequently deposited on to Au substrates in the presence of an intense electric field to promote the deposition of the particles on the surface. For the results presented in this study the DMA was tuned so as to select particles of ion-mobility diameter 30 nm ± 3 nm. Figure 1 shows a scanning electron microscopy (SEM) image of Ag particles on the Au substrate. Particles are evenly distributed across the sample. Coverage of the particles was estimated to be 8%.

Imaging and manipulation were carried out using an ambient AFM/STM (Multimode Nanoscope III, from Veeco, Santa Barbara, CA), and an ultra-high-vacuum (UHV) AFM/STM system (RHK Technology, Troy, MI)[4]. Room cleanliness was better than an equivalent class 1000 standard; room temperature was stabilized at 22 ± 0.1 °C and humidity at 45% ± 5%.

3. Results and discussion

3.1. Scanning probe microscopy imaging

Exhaustive STM imaging of the particle-coated substrates, performed in ambient conditions with a Pt–Ir (70%–30%) tip at various combination of bias voltage (±0.2 to ±5 V) and tunnelling current (1–2 nA), showed only the substrate surface with no evidence of particles. We did not attain imaging conditions for any particular value of bias voltage, as reported earlier [14]. However, following the STM scan, tapping mode AFM images were obtained in the same locations. Tapping mode AFM images of the locations of the prior STM scans are shown in figure 2. The square in the image (4.5 μm × 4.5 μm) (figure 2(a)) is an area of one complete STM scan, whereas the linear patterns (dark bands) in figure 2(b) are created after a few STM scan lines. These patterns confirm that nanoparticles were removed from the scanned locations.

The experiment was also performed in UHV (pressure $< 1 \times 10^{-8}$ Pa) to isolate any environmental effects. Moreover, the pre-amplifier of the UHV STM was capable of achieving
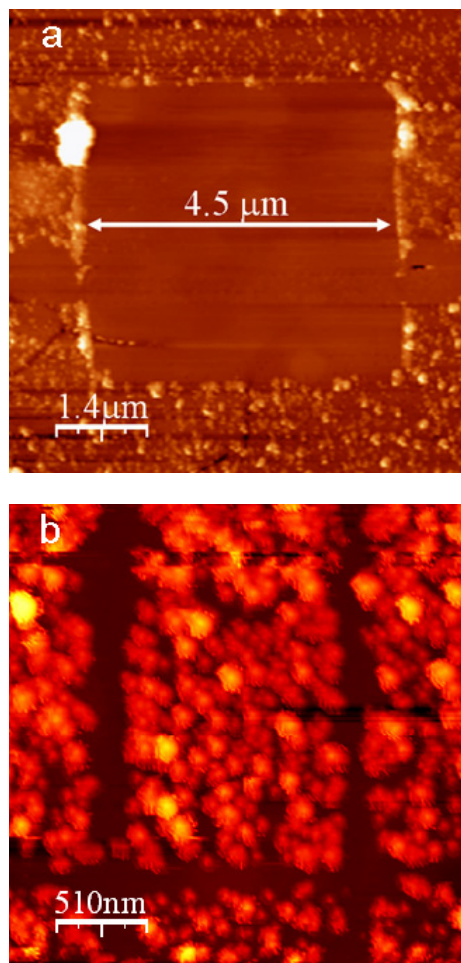
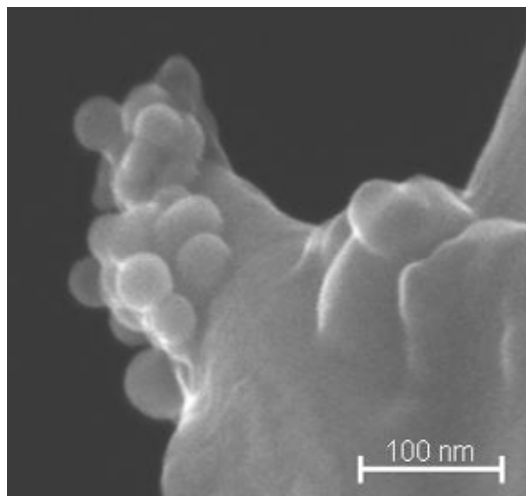**Figure 2.** AFM images (tapping mode) of the location where STM scanning was performed on a Au surface coated with Ag nanoparticles. (a) A location where one full STM scan (4.5 × 4.5 μm^2) is performed (tip bias = 0.2 V, tunnelling current = 1 nA) and (b) a location after a few STM line scans in three locations creating crossing patterns (tip bias = 0.5 V, tunnelling current = 2 nA). STM scan rate was 0.5 Hz for both cases.

tunnelling currents as low as 50 pA, which enabled the tip–particle distance to be increased. Several attempts were made using various tunnelling conditions, and it was evident that a standard imaging protocol using STM always resulted in images of the substrate surface, rather than the particles. It was therefore also evident that the particles were being displaced by some mechanism in the process of imaging. An SEM image (figure 3) of the tip after scanning the surface shows particle agglomeration around the probe.

It is known that contact mode AFM can sweep loosely connected particles aside while scanning [7]. In our experiments, observations showed that particles were mostly collected on the STM tip and removed from the surface. The number of particles collected when scanning large areas is quite large. Hence, there was a tendency toward dropping particles off at the scan boundary where the tip reversed direction. Because of this, some non-uniform pile-up was observed on the boundaries, as can be seen in figure 2(a). It should be noted that the pile-up is not because of a mechanical

Figure 3. SEM image of the STM tip after scanning over the nanoparticle covered surface.

Figure 4. SEM image of a single Ag nanoparticle on an Au surface. The image was taken with a tilt angle of 60° to show the particle contact with the substrate.

dragging of particles to the side, but rather due to a pick-up-drop-off process. Confirming this argument, we do not see any particle pile-up adjacent to small scan areas (figure 2(b)).

STM scanning was found to be rather smooth without any tip crash or sudden jumps caused by high current. This is an indication that the particles jump-on and become attached to the tip and they do not create a conductive path between the tip and the substrate causing a tip crash. There have been some reports of successful imaging of nanoparticles using STM [8], and even using contact mode AFM [15]. A careful comparison of those studies with our results leads to the important conclusion that the particle–substrate adhesion determines the possibility of imaging the particles. Some earlier studies [16] revealed that weakly bound clusters are removed from the scanning area during STM imaging.

The particle–substrate interaction depends on the area of the contacting surfaces and the nature of the two materials. Figure 4 shows an SEM image of a particle on the Au surface obtained with a tilt angle of 60° to get a perspective of the contact between the particle and the surface. The entire spherical profile of the particle and a small contact area are visible. The lower part of the particle appears dark due to low electron emission efficiency from beneath the particle, and hence we expect the contact radius to be even smaller than that observed in the image. Particles prepared by other methods exhibit larger contact areas, and behave like nanoscale islands on the substrate [17–19]. The contact area is an important factor in determining the nature of interactions between the particle and the substrate.

On the other hand, the STM probe–particle interaction is dominated by dielectrophoreis which is a phenomenon arising from the non-uniform electric field of the tip moving adjacent to the surface. The result of this is a net force acting on the particle, enabling it to migrate toward the region of greatest field intensity, which is the STM tip. This force causes nanoparticles to migrate to the region with greater intensity of the field irrespective of the polarity [25], which is consistent with the observation that the particles were being picked up both by a positively and negatively biased tip. The removal of

nanoparticles from the substrate is controlled by the dominance of a dielectrophoretic force between the biased STM probe and the particles over the usual adhesive surface forces between the substrate and the particles. We have analysed these forces, incorporating dielectrophoretic interactions into the contact mechanics of nanoparticle–substrate interactions, in both ambient and ultra-high-vacuum environments.

3.2. Theoretical analysis of interaction forces

Our experiments indicate that particles jump onto the tip at separations larger than the tunnelling distance, suggesting that the substrate–particle force, F_S, is less than the tip–particle force, F_T, at these separations. To confirm this hypothesis, the interaction forces were analysed for the substrate–particle–tip system. The maximum force required to separate the particle from the substrate was calculated using a contact mechanics model based on the superposition of adhesive forces onto those arising from Hertzian contact between a spherical particle and a flat substrate. (Adhesion within the contact area is modelled by the traction field appropriate to uniform displacement, the Johnson–Kendall–Roberts, JKR, model [20]. Adhesion exterior to the contact is modelled by a zone of uniform traction; the combination of JKR with this exterior zone is the so-called Maugis–Dugdale, or MD, model [21].) At the nano-scale, these forces are often sufficient to cause deformation of the contacting surfaces and thereby change the contact area.

The MD model assumes an adhesive potential between the surfaces exterior to the contact that exerts a constant stress, σ_0, until a separation h_0 is reached. The value of h_0 is chosen such that the work of adhesion, $w = \sigma_0 h_0$, matches that of a Lennard-Jones potential describing van der Waals interactions between the surfaces: $w = H/12\pi z_0^2$, where H is the Hamaker constant and z_0 is the distance between the surfaces, such that the stress is given by $\sigma_0 = 0.027 H/z_0^3$ [22]. The Hamaker constant is given by $H = H_{sp} - (H_{sw} + H_{pw} - H_{ww})$, where the subscripts s, p, and w denote substrate, particle, and water, respectively [22]. In UHV, the terms in parentheses are omitted, whereas under ambient conditions the surfaces are covered by an adsorption layer of water and these terms represent the screening of the
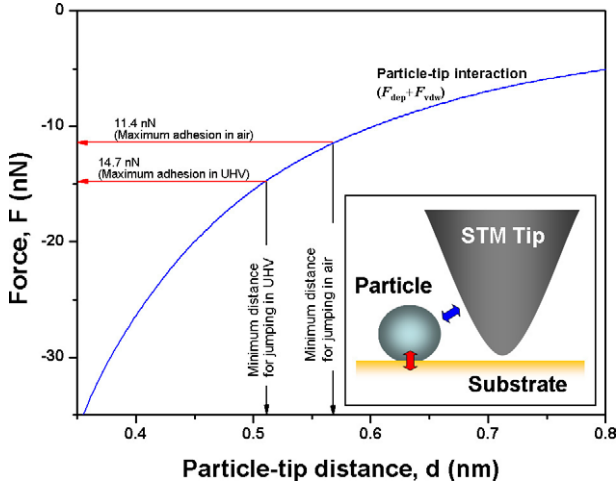
Figure 5. Interaction forces in tip–particle–substrate system during STM imaging. The potential between the STM tip and the particle is assumed to be 0.2 V.

Figure 6. Jumping distance calculated for different particle sizes in UHV and ambient conditions. The potential between the STM tip and the particle is assumed to be 0.2 V.

van der Waals interaction between the substrate and particle by the water interlayer. For Ag and Au, $H(\text{UHV}) = H_{\text{sp}} = 40 \times 10^{-20}$ J and, for water, $H_{\text{ww}} = 3.7 \times 10^{-20}$ J [22]. Estimating $H_{ab} \approx \sqrt{H_{aa} H_{bb}}$ gives the reduced Hamaker constant for the particle and surface under ambient conditions as $H(\text{ambient}) = 19.4 \times 10^{-20}$ J. Using $z_0 = 0.25$ nm as the separation [23] gives $w(\text{UHV}) = 170$ mJ m^{-2}, $\sigma_0(\text{UHV}) = 690$ MPa, $w(\text{ambient}) = 82$ mJ m^{-2}, and $\sigma_0(\text{ambient}) = 335$ MPa. These quantities, along with the particle radius, R, and the reduced modulus of the substrate–particle system, $K = 4/3[(1 - \nu_s^2)/E_s + (1 - \nu_p^2)/E_p]$ (E is Young's modulus and ν is Poisson's ratio of bulk material), allow normalized values of the contact parameters to be defined [21]:

$$A = \frac{a}{(\pi w R^2/K)^{1/3}}, \qquad P = \frac{F}{\pi w R},$$
$$\Delta = \frac{\delta}{(\pi^2 w^2 R/K^2)^{1/3}}, \qquad S = \frac{\sigma_0}{(\pi w K^2/8R)^{1/3}}. \qquad (1)$$

Here a is the contact radius, F is the interaction force, and δ is the displacement of the particle into the surface. The maximum force required to overcome the adhesive interactions and separate the particle from the surface, F_{MD}, is found by simultaneous solution of equations in these normalized coordinates [21]:
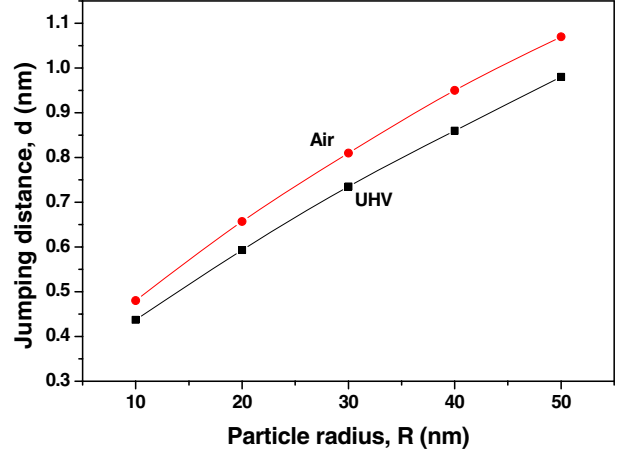
$$P = A^3 - SA^2[C + (C^2 + 1)\tan^{-1} C]$$
$$\Delta = A^2 - 4SAC/3$$
$$(SA^2/2)[C + (C^2 - 1)\tan^{-1} C] + (4S^2A/3) \qquad (2)$$
$$\times [C\tan^{-1} C + 1 - (C^2 - 1)^{1/2}] = 1,$$

where $C = [(c/a)^2 - 1]^{1/2}$ and c is the radius where the separation between the two surfaces reaches h_0. The first terms in the P and Δ equations above represent the Hertzian response and the second terms the modifications of the MD model accounting for adhesive interactions between the surfaces.

For a 15 nm radius Ag particle on a Au substrate we find $F_{\text{MD}}(\text{UHV}) = F_S(\text{UHV}) = 14.7$ nN and $F_{\text{MD}}(\text{ambient}) = 7.4$ nN. Under ambient conditions, a capillary force associated

with the condensation of a water meniscus around the substrate–particle interface,

$$F_{\text{cap}} = 4\pi \gamma_w R \cos\theta \qquad (3)$$

must be included [22], where γ_w is the surface tension of water (73 mJ m^{-2} at 20 °C) and $\theta = 73°$ is the wetting angle. We find $F_{\text{cap}} = 4$ nN and thus $F_S(\text{ambient}) = F_{\text{MD}}(\text{ambient}) + F_{\text{cap}} = 11.4$ nN.

Tip–particle attractive forces were calculated as a function of the separation, d, between a nanoparticle and the STM tip, with the assumption that there was no residual charge on the particle. The bias voltage between the tip and a nanoparticle generates an electric field, $E(d)$, that induces a dielectrophoretic force, F_{dep}, and an image force, F_i, between the tip and the particle. Assuming the particle is small relative to any curvature of the electric field, these two forces are

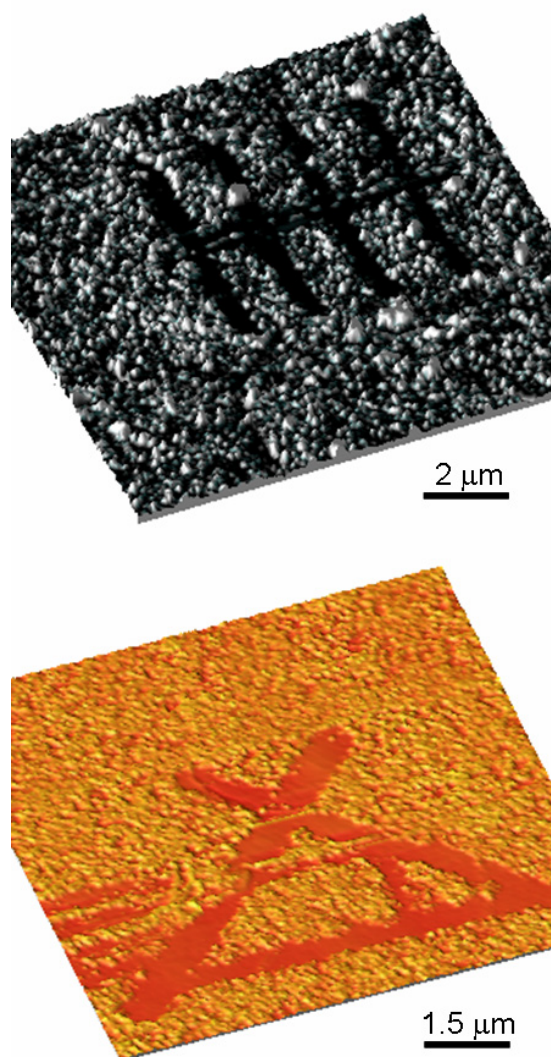$$F_{\text{dep}}(d) = 4\pi \varepsilon_0 \varepsilon_m R^3 E \cdot \nabla E \qquad (4)$$

$$F_i(d) = -\pi \varepsilon_0 \varepsilon_m R^2 E^2 \qquad (5)$$

where ε_0 is the permittivity of free space and ε_m is the relative permittivity of the medium between the particle and tip [24, 25]. Taking $\varepsilon_m = 1$ and using a bias voltage of 0.2 V, we find $F_i \approx 0.5$ nN at minimal separation, leaving $F_{\text{dep}}(d)$ as the dominant electrical force in the non-uniform electric field. Van der Waals interactions between the tip and particle are given by

$$F_{\text{vdW}} = -H_{\text{tp}} R/6d^2 \qquad (6)$$

where $H_{\text{tp}} = 40 \times 10^{-20}$ J. The total force exerted by the tip on the particle is thus given by $F_T(d) = F_{\text{dep}}(d) + F_{\text{vdW}}(d)$.

The resultant forces from van der Waals and dielectrophoretic interactions between the STM tip and a particle are shown as a function of tip–particle separation in figure 5. The minimum tip–particle separation necessary to overcome the maximum adhesion between a particle and the substrate is around 0.51 and 0.57 nm for UHV and ambient conditions, respectively. As nanoparticles were not observable by STM, we presume that these separations are larger than the tunnelling

we conclude that there is little material effect for metallic nanoparticles.

These results indicate that the particle–substrate interaction needs to be controlled for STM imaging of nanoparticles. In order to overcome the force generated by the tip, one needs to increase the adhesion of the particle to the substrate and this can be achieved by changing the contact area of the particle with the substrate. Thermal annealing should help to increase the contact area and thereby enhance the particle–surface bond sufficiently to overcome the interactions with the scanning probe [7]. Chemical modifications of the surfaces have also found to be effective in immobilizing the nanoparticles on the substrates [28]. Stronger particle–substrate interaction will enable a closer approach of the tip for imaging without particles being removed.

The nanoparticle–substrate system used in these experiments is an ideal case for controlled lithography. Because of the loose attachment, it was possible to create various shapes on the substrate by moving nanoparticles and creating particle-free zones. Figure 7 illustrates the ability to create particle-free areas in a controlled way. This technique offers nanoparticle-based technology for organizing and patterning of surfaces for various applications.

4. Conclusion

STM studies show that the imaging and manipulation of nanoparticles depend on the particle-substrate adhesion. For imaging, particles need to be connected strongly to the surface, whereas for soft-landed particles using an approach similar to that described in this work, particles can be moved selectively. The mechanism of particle removal from the surface using STM was analysed in terms of contact mechanics and electrostatics, and the calculations show that there is sufficient force for the nanoparticles to jump onto the tip before tunnelling occurs. This offers the possibility for performing lithography on the surface as demonstrated. Our studies emphasize the importance of particle–substrate adhesion as determined by synthesis and preparation methods.

Figure 7. Illustration of the capability of STM nanoparticle lithography to create structures on surfaces. Images were obtained using tapping mode AFM.

distance between particle and tip. The tunnelling distance in STM depends on various factors such as the electron work-function of the materials, bias voltage, and the shape of the tip, and in typical imaging conditions varies from a couple of angstroms to a nanometer, depending on the electrical properties of the material [26]. The tunnelling distance between materials like Au–W in clean ultra-high-vacuum conditions can be 0.6 nm [27]. The tunnelling distance for our samples is expected to be smaller due to the poor nanoparticle–substrate contact because of the native adsorption layer. Hence we expect that the nanoparticles jump from the substrate to the STM tip before reaching the tunnelling contact.

Calculations for increasing particle sizes show an increase in the magnitude of the dielectrophoretic forces in comparison with the adhesion forces (figure 6). This means that larger particles can jump a greater distance. Furthermore, different combinations of metallic nanoparticles and substrates do not show any noticeable variation in our calculations, and hence

References

[1] Lin Y *et al* 2005 *Nature* **434** 55
[2] Rabani E, Reichman D R, Geissler P L and Brus L E 2003 *Nature* **426** 271
[3] Yun S-H, Sohn B-H, Jung J C, Zin W-C, Ree M and Park J W 2006 *Nanotechnology* **17** 450
[4] Xia Y, Rogers J A, Paul K E and Whitesides G M 1999 *Chem. Rev.* **99** 1823
[5] Lyuksyutov S F, Vaia R A, Paramonov P B, Juhl S, Waterhouse L, Ralich R M, Sigalov G and Sancaktar E 2003 *Nat. Mater.* **2** 468
[6] Zamborini F P, Smart L E, Leopold M C and Murray R W 2003 *Anal. Chim. Acta* **496** 3
[7] Junno T, Anand S, Deppert K, Montelius L and Samuelson L 1995 *Appl. Phys. Lett.* **66** 3295
[8] Sily F, Gusev A O and Charra F 2004 *Appl. Phys. Lett.* **79** 4013
[9] Scheier P and Sattler K 2003 *Eur. Phys. J.* D **24** 347
[10] Krinke T J, Deppert K, Magnusson M H and Fissan H 2002 *Part. Part. Syst. Charact.* **19** 321
[11] Pluym T C, Powell Q H, Gurav A S, Ward T L, Kodas T T, Wang L M and Glicksman H D 1993 *J. Aerosol Sci.* **23** 383
[12] Kim S H and Zachariah M R 2005 *Nanotechnology* **16** 2149

[13] Tsai D-H, Kim S H, Corrigan T D, Phaneuf R J and
     Zachariah M R 2005 *Nanotechnology* **16** 1856
[14] Rolandi M, Scott K, Wilson E G and Meldrum F C 2001
     J. Appl. Phys. **89** 1588
[15] Harel E, Meltzer S E, Requicha A G, Thompson M E and
     Koel B E 2005 *Nano Lett.* **5** 2624
[16] Hövel H, Becker T H, Bettac A, Reihl B, Tschudy M and
     Williams E J 1997 *J. Appl. Phys.* **81** 154
[17] Song Z, Hrbek J and Osgood R 2005 *Nano Lett.* **5** 1327
[18] Hata K, Futaba D N, Mizuno K, Namai T, Yumura M and
     Iijima S 2004 *Science* **306** 19
[19] Liu D F *et al* 2005 *Nanotechnology* **16** 2665
[20] Johnson K L, Kendall K and Robert A D 1971 *Proc. R. Soc.* A
     324 301
[21] Maugis D 1992 *J. Colloid Interface Sci.* **150** 243
[22] Israelachvili J N 1991 *Intermolecular and Surface Forces*
     (London: Academic)
[23] Israelachvili J N and Pashley R M 1983 *Nature* **306** 249
[24] Krinke T J, Deppert K, Magnusson M H, Schmidt F and
     Fissan H 2002 *J. Aerosol Sci.* **33** 1341
[25] Kadaksham A T J, Singh P and Aubry N 2004 *Electrophoresis*
     25 3625
[26] Binnig G and Rohrer H 1982 *Helv. Phys. Acta* **55** 726
[27] Sun Y, Mortensen H, Schar S, Lucier A-S, Miyahara Y,
     Grutter P and Hofer W 2005 *Phys. Rev.* B **71** 193407
[28] Yang G, Tan L, Yang Y, Chen S and Liu G Y 2005 *Surf. Sci.*
     589 129